

人体、服装、环境系统动态热湿传递数值模拟

刘迎曦 李凤志

罗钟铉

李毅

(大连理工大学工程力学系, 大连, 116024)

(大连理工大学应用数学系)

(香港理工大学纺织及制衣学系)

摘要: 建立了人体—服装—环境系统的动态热湿传递模型。对 Stolwijk 人体热调节模型进行了改进, 考虑到了汗水的积聚过程, 并结合织物热湿耦合模型, 用于人、服装、环境系统的瞬态热湿传递过程的数值模拟。在模型中, 考虑了纤维对湿的吸附与解吸过程及其对热传导率、热容的影响, 以及相变导致的热生成及释放。实验表明了模型的良好预测性能。

关键词: 人体热调节 热湿耦合模型 数值模拟 服装 环境系统

中图分类号: TS 941.15

文献标识码: A

文章编号: 0253-9721(2004)05-0024-04

应用数学模型模拟人体热湿行为, 已广泛地应用于医学、航空、航天、潜水、空调设计、“人一机—环境”系统工程等各个领域。本文的研究是从地球环境下人体着装舒适性的角度出发的。

人体热调节数学模型, 由简单的一点模型^[1]、两点模型^[2,3] 逐渐发展成多结点模型^[4-6]、多单元模型^[7,8]。以 Stolwijk^[4] 模型为代表的多结点模型, 以计算简单、精度可以满足工作需要而在工程中得以广泛采用。但 Stolwijk 模型未能考虑皮肤表面汗水积聚, 认为人体分泌的汗液全部蒸发, 这样的着装条件是不符合实际的。汗水在人体表面的积聚对人体的热湿舒适感的评价有直接的影响, 应该给予考虑。人体热调节模型提出后, 为了考虑服装对人体的影响, 早期研究者^[2] 采用对传输系数乘以服装影响因子的方法, 考虑比较粗糙。近期研究者^[7,8] 应用 Farnworth^[9] 提出的服装整体模型, 与人体热调节模型进行联合, 实现了动态模拟, 但 Farnworth 服装整体模型是一个热阻和湿阻模型, 未能考虑纤维吸附(解吸)水分对导热系数及热容的影响。

纤维对湿的吸附与解吸, 是服装热湿舒适性研究所要考虑的核心问题。一方面, 纤维对湿的吸附与解吸要放热和吸热; 另一方面, 纤维含水量对吸湿性较大的纤维组成的织物的导热系数及热容有重要影响^[10]。对着装的动态热湿舒适性研究来说, 这两方面的影响都是不容忽略的, 在模拟中应当很好地给予考虑。

针对上述问题, 本文对 Stolwijk 模型进行了改进, 并且结合服装热湿耦合模型, 对人、服装、环境系统进行了动态数值模拟。

1 人体热湿调节系统数学模型

在 Stolwijk 人体热调节模型中, 人体的热系统分为被动系统和主动系统两个部分。

1.1 被动系统

人体被动系统由 6 个圆柱(球)节段(头、躯干、臂、手、腿和足)组成。每一个圆柱(球)节段又分成 4 层: 内核、肌肉、脂肪和皮肤。每一层假设具有相同的温度, 故每一层可以看做一个点。循环系统通过一个中心血池同每一部分连接, 表示大动脉、静脉。中心血池同每一部分的热交换是通过血液流动以对流的方式进行的。中心血池也可以看做一个点, 故该模型也称之为 25 节点人体热调节模型。

对于每一层, 热平衡方程可以写成如下形式:

$$C_{p,n} \frac{dT_n}{dt} =$$

$$M_n - B_n - K_n - R_n - C_n - (E_n + E_{res})$$

$$n = 1, 2, \dots, 24 \quad (1)$$

式中, 下标 n 表示第 n 个组织层, $C_{p,n}$ 表示热容 ($W \cdot s / ^\circ C$), T_n 表示温度 ($^\circ C$), t 是时间 (s), M_n 表示代谢热生成 (W), B_n 表示血液流动引起的热损失 (W), K_n 、 R_n 、 C_n 分别为传导、辐射、对流引起的热损失 (W), E_n 、 E_{res} 分别表示由皮肤表面蒸发和呼吸引起的热损失 (W)。在 Stolwijk 模型中认为人体分泌的汗液全部蒸发, 忽略了汗水在人体表面的积聚, 这在着装人体上是不符合实际的。本文采用 Jones^[9] 提出的汗水积聚计算方法对 Stolwijk 模型进行改进, 由皮肤表面向周围环境蒸发的热量由下式计算:

$$E_i = \frac{P_{sk,i} - P_{ea,i}}{R_{ea,i}} S_i \quad (2)$$

式中, 下标 i 表示第 i 个节段, $P_{sk,i}$ 、 $P_{ea,i}$ 分别表示第 i 个节段处皮肤表面和皮肤周围环境的水蒸汽分压 (Pa), S_i 为第 i 个节段的面积 (m^2), $R_{ea,i}$ 表示第 i 个节段处皮肤表面空气层的蒸发热阻 ($m^2 \cdot Pa / W$)。当

国家自然科学基金资助项目(10072014), 高校博士点专项基金资助项目(2000014107)。

皮肤表面没有汗积聚时^[6],

$$P_{sk,i} = \frac{P_{sat,i}R_{ea,i} + P_{ea,i}R_{esk} + m_{rsw}h_{fg}R_{ea,i}R_{esk}}{R_{ea,i} + R_{esk}} \quad (3)$$

(如果 $P_{sk,i} > P_{sat,i}$ 那么 $P_{sk,i} = P_{sat,i}$)

式中, $P_{sat,i}$ 表示第 i 个节段处皮肤温度下的饱和蒸汽压(Pa), R_{esk} 表示皮肤蒸发热阻($m^2 \cdot Pa/W$), m_{rsw} 皮肤出汗率($kg/s \cdot m^2$), h_{fg} 表示蒸发潜热系数(J/kg)。当皮肤表面由汗液积聚时,

$$P_{sk,i} = P_{sat,i} \quad (4)$$

汗液积聚过程由下式描述^[6]:

$$\frac{dm_{s,i}}{dt} = m_{rsw} + \frac{P_{sat,i} - P_{sk,i}}{R_{esk}h_{fg}} - \frac{P_{sk,i} - P_{ea,i}}{R_{ea,i}h_{fg}} \quad (5)$$

其中, $m_{s,i}$ 表示第 i 个节段处皮肤表面汗积聚量(kg/m^2)。

对于中心血池:

$$c_b \frac{dT_b}{dt} = \sum_{n=1}^{24} B_n \quad (6)$$

其中, c_b 是血液的热容量($W/s \cdot ^\circ C$), T_b 是中心血池温度($^\circ C$)。

1.2 主动系统

人体的热生理活动包括血管运动、汗腺活动、代谢产热、寒颤产热等,通过调节热生理活动的水平,实现产热和散热的动态平衡,维持体温的相对稳定。Stolwijk 模型以人体热中性状态温度为基准,将第一组织层瞬态温度同基准温度的差函数,作为人体热调节控制指令的控制变量。中枢及皮肤感受器根据下式获得误差信号:

$$e_n = (T_n - T_{n,set}) \quad (7)$$

随即可以确定“冷”或“暖”输出,在获得头核温度信号和综合皮肤冷暖信号的基础上,效应器产生整体出汗或打颤、血管收缩或舒张 4 种反应量,根据以上的整体输出,调节器来调节每一部分人体代谢率、血流量及出汗量,实现体温调节,详细过程参见文献[4]。

2 服装系统热湿传输数学模型

对于服装系统热湿传递,本文采用热湿耦合模型,该模型由 Henry^[11] 首先提出,经过 Nordon^[12] 及 Li^[10,13] 和 Luo^[14] 等人的发展,可以很好地描述织物的热湿传输机理。本文采用改进后的热湿耦合模型。

2.1 热平衡方程

$$C_v \frac{\partial T}{\partial t} - \lambda(1 - \epsilon) \frac{\partial C_f}{\partial t} = \frac{\partial}{\partial x} \left[K \frac{\partial T}{\partial x} \right] \quad (8)$$

2.2 质量守恒方程

$$\epsilon \frac{\partial C_a}{\partial t} + (1 - \epsilon) \frac{\partial C_f}{\partial t} = \text{div}(-\vec{m}_a^D) \quad (9)$$

其中, ϵ 为孔隙率, C_a 为纤维间孔隙中的蒸汽浓度(kg/m^3), C_f 为纤维中的蒸汽浓度(kg/m^3), T 是温度($^\circ C$), C_v 、 λ 、 K 分别为织物的体积热容量($J/m^3 \cdot ^\circ C$)、吸附热(J/kg)、热传导系数($W/m \cdot ^\circ C$),它们是纤维中含水量和温度的函数。纤维中水的积聚率符合 Fick 定律^[13]:

$$\frac{\partial C_f'}{\partial t} = \frac{1}{r} \frac{\partial}{\partial r} \left[r' D_f(W_c, t) \frac{\partial C_f'}{\partial r} \right] \quad (10)$$

其中, C_f' 是纤维中的湿浓度(kg/m^3), $D_f(W_c, t)$ 是纤维内蒸汽扩散率(m^2/s),是含水量 W_c 和时间 t 的函数,是一个两阶段变化系数。其中含水量 W_c 由下式确定:

$$W_c(x, t) = C_f(x, t) / \rho \quad (11)$$

其中, C_f (kg/m^3)是 C_f' 在 $[0, R_f]$ 范围内的平均值, ρ 是纤维密度(kg/m^3)。

纤维的边界条件由下式确定:

$$C_f'(R_f) = f(RH, T) \quad (12)$$

其中, C_f' 是纤维表面的湿浓度(kg/m^3), f 是与空气相对湿度及温度相关联的非线性函数,它可以通过纤维吸湿(解吸)等温曲线确定。

水蒸汽的质量流率 \vec{m}_a^D 由下式确定^[15]:

$$\vec{m}_a^D = -1.952 \times 10^{-7} \epsilon \times \frac{T^{0.8}}{P_g - P_a} \text{grad} P_a \quad (13)$$

其中, P_g 为大气压力(Pa), P_a 为水蒸汽分压(Pa)。

2.3 边界条件

人一服装—环境系统示意图如图 1 所示,服装层与皮肤之间是空气层。

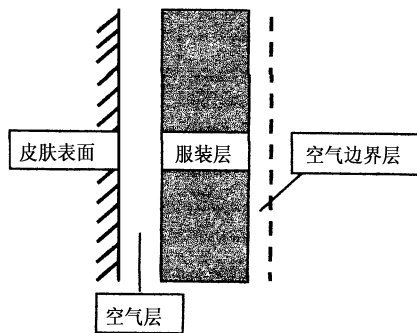


图1 人一服装—环境系统示意图

第 i 个节段处服装左端(靠近皮肤处)边界条件为:

$$\vec{m}_a^D |_{\text{left},i} = \frac{1}{R_{ea,i}h_{fg}} (P_{\text{atd},i} - P_{sk,i}) - K \text{grad} T |_{\text{left},i} = \frac{1}{R_{ea,i}} (T_{\text{left},i} - T_{sk,i}) +$$

$$\frac{1}{R_{ea,i}}(P_{a\text{left},i} - P_{sk,i}) \quad (14)$$

第 i 个节段处服装右端(靠近环境处)边界条件为:

$$\begin{aligned} \dot{m}_a^D \Big|_{\text{right},i} &= \frac{1}{R_{a1,i} h_{fg}}(P_{a\text{right},i} - P_{a\infty,i}) - \\ K_{\text{grad}T} \Big|_{\text{right},i} &= \frac{1}{R_{a1,i}}(T_{\text{right},i} - T_{\infty,i}) + \\ &\frac{1}{R_{a1,i}}(P_{a\text{right},i} - P_{a\infty,i}) \end{aligned} \quad (15)$$

式(13)、(14)边界条件中,下标 left, right 分别表示服装左、右边界点, i 表示人体的第 i 个节段, ∞ 表示服装周围环境。服装微气候内的空气层中干热流有两个并行途径,一是通过空气的传导,另一个是在织物表面间的辐射。因此第 i 个节段处皮肤与服装间空气层的热阻 $R_{a,i}$ ($^{\circ}\text{C}\cdot\text{m}^2/\text{W}$)可用下式表示^[16]:

$$R_{a,i} = \frac{1}{h_r + k/t_{a,i}} \quad (16)$$

辐射热传输系数 h_r 和空气的导热系数 k 的值选用文献[16]中的结果 $h_r = 4.9 \text{ W}/\text{m}^2\cdot^{\circ}\text{C}$ 及 $k = 0.024 \text{ W}/\text{m}\cdot^{\circ}\text{C}$ 。 $t_{a,i}$ 为第 i 个节段处皮肤与服装间的空气层厚度(mm)。

根据文献[16],第 i 个节段处皮肤与服装间蒸汽的蒸发热阻 $R_{ea,i}$ ($\text{m}^2\cdot\text{Pa}/\text{W}$)为指数形式:

$$R_{ea,i} = a[1 - \exp(-t_{a,i}/b)] \quad (17)$$

其中, a, b 为常数, $a = 33.4 \text{ m}^2\cdot\text{Pa}/\text{W}$, $b = 15 \text{ mm}$, $t_{a,i}$ 为第 i 个节段处皮肤与服装间的空气层厚度(mm)。

暴露于环境中的外表面边界层的热阻和蒸发阻力略有不同,热阻^[16]:

$$R_{a1,i} = \frac{1}{h_r + h_{c,i}} \quad (18)$$

辐射热传输系数 h_r 的值为 $4.9 \text{ W}/\text{m}^2\cdot^{\circ}\text{C}$ 。如果空气层移动,对流热传输系数 $h_{c,i}$ 是速度的函数。外层空气蒸发热阻可以由对流热传输系数 Lewis 关系给出^[16]:

$$R_{ea1,i} = \frac{1}{h_{c,i} LR} \quad (19)$$

2.4 初始条件

$$T = T_0, C_a = C_{a0}, C_f' = f(RH_0, T_0) \quad (20)$$

3 计算步骤

1)对于人体热平衡方程采用简单的方法,根据初始的代谢量、血管的收缩及舒张量、出汗量、打颤热生成量、皮肤表面的汗水积聚量以及服装表面的温度、湿浓度等,由方程(1)及方程(6)计算每一时刻、每一个节点的能量变化率,由方程(5)计算每一时刻、每一节点的汗水积聚率,然后通过前一时刻该点的温度、汗水积聚量,求出当前时刻该点的温度、汗水积聚量。根据当前步的温度可以计算新的调节量。为了保证计算结果的稳定性,控制计算时间步长使得每一计算步温度变化最大不超过 0.1°C 。计算 10 s 后输出结果。

2)对于服装热湿耦合方程(8)、(9)空间上应用有限体积方法离散,时间域应用隐式格式离散,根据前一时刻的服装初始温度、湿浓度、纤维含水量以及相应皮肤和环境的边界条件可以求得当前时刻的服装温度、湿浓度。计算 10 s 后输出结果。

3)每隔 10 s 后,更新人与服装的边界条件开始新的计算。

4 模型验证及预测

为了验证着装人体模型的热湿预测性能,利用文献[18]的实验数据,与本文模型预测结果进行了比较。实验研究对象为 3 个健康的大学生,穿 T 恤衫、裤子。服装均为纯棉制作,厚度 2.2 mm,孔隙率为 0.67。初始时刻,人在 A 室(温度 25°C ,空气相对湿度 40%,空气速度为 $0.3 \text{ m}/\text{s}$)静坐 15 min,使人服装环境达到平衡状态,然后进入 B 室(温度 36°C ,空气相对湿度 80%,空气速度为 $0.1 \text{ m}/\text{s}$)开始计时,静坐 20 min,然后回到 A 室,静坐 40 min。人体物性参数及热调节控制参数详见文献[4],服装材料特性见表 1。

实验和本文理论预测结果如图 2~4 所示。

表 1 服装材料特性

特性	符号	单位	(纯棉)物性参数表达式
纤维中水蒸汽扩散系数	第一阶段	D_f	$(0.85 + 50.6W_c - 1100W_c^2) \times 10^{-14}, t < 540 \text{ s}$
	第二阶段	D_f	$2.5\{1 - \exp[-3.5 \exp(-45W_c)]\} \times 10^{-14}, t \geq 540 \text{ s}$
织物的体积热容	C_v	$\text{kJ}/\text{m}^3\cdot^{\circ}\text{K}$	$(1663.0 + 4184.0W_c)/(1 + W_c)$
织物的热传导率	K	$\text{W}/\text{m}\cdot^{\circ}\text{K}$	$(44.1 + 63.0W_c) \times 10^{-3}$
吸附热	λ	kJ/kg	$1030.9 \exp(-22.39W_c) + 2522.0$
纤维密度	ρ_f	kg/m^3	1550
纤维半径	R_f	m	1.03×10^{-5}

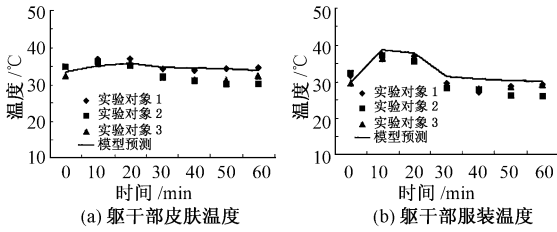


图2 着装部分(躯干)皮肤及服装温度理论预测与实验结果比较

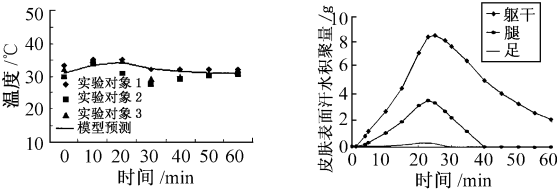


图3 裸露部分(臂)温度理论预测与实验结果比较

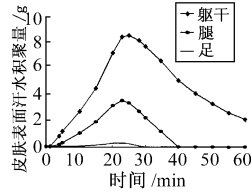


图4 皮肤表面汗水积聚量随时间变化的理论预测

从图2(a)可以看出,被服装覆盖的躯干部温度在最初20 min升高,在后40 min逐渐降低。这是由于环境的变化及人体热调节的影响。

图2(b)指出躯干部服装温度分布,初始阶段(0~12 min)温度上升是由两方面原因引起的,一方面是环境温度的升高(由25℃到36℃),另一方面是环境湿度变化引起,由于从湿度低的条件到湿度高的条件纤维吸湿放热使服装温度升高。从12 min到20 min后温度降低,这是由于随着纤维吸湿率的降低,外界环境与服装之间的热交换量占主导地位,使服装温度降低。从图2(b)中还可以看出纤维的吸湿对服装温度的影响,服装两侧温度在35~36℃之间,利用吸湿产生的潜热,使服装温度提高了大约3℃,这是由于棉的吸湿性较高的缘故,也是为什么服装动态舒适性研究要考虑纤维的吸附与解吸的原因。

图3显示了由于穿T恤衫裸露的臂部温度的实验值和预测值的比较结果。从图2和图3可以看出,本文的理论预测趋势同实验值的趋势相近,其预测数值精度能够满足工程需要。

图4给出了模型预测的标准人体在不同部位的皮肤表面汗水积聚量,可以看出,胸部皮肤汗水积聚较多,其次是腿和脚。从图4中可以看到,汗水积聚的峰值略滞后于20 min处,这是因为刚从B室到A室,人体仍然出汗,且出汗率大于蒸发率,随着时间的推移,环境温度变冷,皮肤出汗率减少,汗液逐渐蒸发减少。

5 结语

建立了人—服装—环境系统的热湿传递过程的

数学模型,从织物的传热传质的基本机理出发,从最基本的单位(纤维)考虑起,并与人体热调节模型相结合,通过理论与实验的对比,看出该模型的可行性。

参考文献

- Givoni B et al. Predicting Rectal Temperature Response to Work, Environment and Clothing. *J. Appl. Physiol.*, 1972(34): 201~204.
- Gagge A P. An Effective Temperature Scale Based on a Simple Model of Human Physiological Regulatory Response. *ASHRAE Trans.* 1971(77): 247~262.
- Madler W et al. Heat; Man's Exchanges and Physiological Responses. *Physiol. Rev.*, 1947(27): 200~227.
- Solwijk J. A. J et al. Control of Body Temperature. *Handbook of Physiology- Reaction to Environmental Agents* 1977; 45~67.
- Grosbie R. J et al. Electrical Analog Simulation of Temperature Regulation in Man. *Temperature- Its Measurement and Control in Science and Industry*, 1963(3): 627~635.
- Jones B. W et al. Transient Interaction between the Human and the Thermal Environment. *ASHRAE Trans.*, 1992(98): 189~195.
- Wissler E. H et al. Mathematical Simulation of Human Thermal Behavior Using Whole Body Models. In: *Heat and Mass Transfer in Medicine and Biology*. 1985, Plenum.
- Smith C. E et al. A Transient, Three-dimensional Model of the Human Thermal System. *Kansas State University*. 1991.
- Farnworth B et al. A Numerical Model of the Combined Diffusion of Heat and Water Vapor through Clothing. *Text. Res. J.*, 1986(56): 653~664.
- Y. Li et al. A Two-stage Sorption Model of the Coupled Diffusion of Moisture and Heat in Wool Fabric. *Textile Res. J.*, 1992(4): 211~217.
- Henry P. S. H. The Diffusion of Moisture and Heat Through Textiles. *Discuss. Faraday Soc.*, 1948(3): 243~257.
- Nordon H. G. D. A. P. Case Studies of Coupled Heat and Moisture Diffusion in Wool Beds. *Textile Res. J.*, 1969(39): 166~172.
- Y. Li et al. An Improved Mathematical Simulation of the Coupled Diffusion of Moisture and Heat in Wool Fabric. *Textile Research Journal*, 2000.
- Zhongxuan Luo et al. Heat and Moisture Transfer with Sorption and Condensation in Porous Clothing Assemblies and Numerical Simulation. *International Journal of Heat and Mass Transfer* 2000(43): 2989~3000.
- Li Fengzhi et al. Numerical Simulation of Coupled Heat and Mass Transfer in Hygroscopic Fabrics Considering the Influence of Atmospheric Pressure. *Numerical Heat Transfer, Part B* 2004(45): 249~262.
- Yigit A. The Computer-based Human Thermal Model. *Int. Comm. Heat Mass Transfer*, 1998(7): 969~977.
- Xiaojiang Xu et al. A Dynamic Model of the Human/Clothing/Environment-system. *Appl. Human Sci.*, 1997(2): 61~75.
- Tetsuya Umeno et al. Prediction of Skin and Clothing Temperatures under Thermal Transient Considering Moisture Accumulation in Clothing. *ASHRAE Trans.*, 2001(107): 71~81.

JOURNAL OF TEXTILE RESEARCH

(Bimonthly)

Vol. 25, No. 5, Sum 230, Oct. 2004

Contents

(Abstracts Inc.)

Research Reports

Structure and Processing Properties of the Natural Colored Cotton

The reasons of instabilities of size, colorant and poor spinning property of the natural colored cotton has been analyzed in the respect of structure in order to offer the reference for industrial production. Zhang Mei *et al* (7)

Preparation and Mechanical Properties of Fibroin/Sericin Blended Film

The fibroin/sericin blended films were prepared with epoxides resins as cross-linking agent. The properties and structure of blended films was investigated. Results show that the blended film, which prepared by 10% fibroin and 90% sericin, PEGO 4-1 as cross-linking agent, has better physical and mechanical properties. Xie Ruijuan *et al* (10)

Study on Cross-linking Properties Between Cotton and Chitosan

Treat cotton knitted fabric with poly-carboxylic acid and chitosan as finishing agent. Study on the properties of cross-linking by the technique of Fourier Transform Infrared Spectrum and X-ray Photoelectron Spectrometry. Results show that the cross-linking takes place between cotton and chitosan in the presence of cross linking agents. Xu Yunhui *et al* (12)

Study on Surface Modification of Soybean Protein Fiber with DBD Plasma

Treat soybean protein fiber and its roving with Dielectric Barrier Discharge (DBD) technique, that can change their surface morphology significantly and increase the frictional coefficient of the soybean, thus improve the cohesion force of the soybean protein fiber in roving, at meanwhile there is no significant change in strength and elongation of soybean protein fiber. Wu Huijeng *et al* (15)

Study on Dyeing Properties of Polyester with Disperse Dyes in Supercritical Carbon Dioxide

Dynamic characteristics of PET fiber dyed with Disperse Blue C. I. 79 in supercritical carbon dioxide medium was studied. Its diffusion coefficients and the activation energy of different temperature in such situation were obtained. Hou Aiqin *et al* (17)

Research on Dyeing Properties of Coloring Material from Carthamin on Ramie and Natural Silk Fabrics

Analyze and compare the dyeing properties of carthamin and safflower yellow on ramie and natural silk. The K/S value of safflower yellow on natural silk is much higher than that on ramie and has different color eigenvalue from ramie, and the K/S value of carthamin on natural silk is close to it on ramie, but it has different color eigenvalue from ramie. Metal ions will affect the stability of carthamin. Yu Zhicheng (19)

Determination of Free Formaldehyde in Textiles by High Performance Liquid Chromatography

Set up the liquid chromatography method for determining hydrolyzed free formaldehyde in textiles. The formaldehyde in textiles is extract in water and reacted with 2,4-dinitro-phenylhydrazine. Its derivative compound can be analyzed directly without any other solvent. So the method is simple, quick and economical. The conventional syngenic chemicals have no interference. Recover ratio is 93%~103%. Chen Haixiang *et al* (21)

Numerical Simulation of Dynamic Heat-moisture Transfer within the Human-Clothing-Environment System

Establish the Stolwijk's human thermal regulatory model, take the accumulative course of perspiring into consideration, then combine the heat-moisture transfer model of fabric for numerical simulation of instantaneous status heat-moisture transfer course in human-clothing-environment system. The phenomenon that the fiber can adsorb and desorb moisture is the problem at core on study into the comfort property of clothes which is bound up with dynamic heat-moisture transfer. The effects of the thermal conductivity rate, thermal capacity as well as heat occur and release due to phase change also be taken in consideration as the model set up. Experiments show the model possess a good predictability. Liu Yingxi *et al* (24)

Analysis and Investigations

Study on Identification of Bamboo Fiber

Base on the well-know knowledge of the elementary physical properties of bamboo fiber and viscose fiber, identify these two kinds of fiber effectively by three methods, i. e. observing fiber microstructure, measuring lignin content and the infrared spectrum, to analyze and compare bamboo fiber and viscose fiber. Zhang Tao *et al* (28)

Preparation and Property of Anti-ultraviolet Polyamide Chip

Test the nanometer SiO_2 and TiO_2 by TEM. After surface modification, these two nano-materials were mixed together with powdered polyamide in proportion, extruded and chipped, then made into film. Test its transparency of ultraviolet by UV-spectrophotometer and the properties of anti-ultraviolet of polyamide chip. Discuss the factors that affect the anti-ultraviolet properties of polyamide chip. Qian Jianhua *et al* (30)

Weighting Properties of Mulberry Silk after the Plasma Treatment

Stannic acid is used to characterize the voids felling capacity in silk fiber after the mulberry silk fiber was treated with low temperature oxygen plasma. Results show that the plasma treatment makes the stannic acid gel fill in the inner part of the silk easily and improves its weighting ability, which indicates the micro-voids appear in the silk. The aggregate structure of silk fiber treated with plasma changes and crystalline degree of it decrease after stannic acid weighting treatment. Ren Yu *et al* (32)

Prediction of the Quality of Worsted Yarn

Prediction of the quality of worsted yarn including the parameters such as evenness, thin place, thick place, yarn tenacity and elongation at break etc., by Multi-Layer Perceptron (MLP) and Levenberg-Marquardt (LM) algorithm. The experiment shows that there is high correlation between the predictive value and measured value of yarn quality, which indicates the MLP model and LM algorithm can be used in practical prediction of worsted yarn quality. Wang Kanfeng *et al* (34)

Study on Varying Principle of Fiber Property in Pure Cotton Card Sliver Making Process

Thirty pure card slivers were made of different components from ten Chinese medium cotton, and test with HVI 900 system. The varying principle of fiber properties in the process was investigated. It will be of reference value to cotton assorting in cotton mill. Zhang Hongwei (36)

Application of New Method Spinning Nu-Torque™ Yarn for Weaving

Put a attachment on conventional ring spinning frame, a lower torsion moment yarn (Nu-Torque™ yarn) was produced by this new spinning method. 100% cotton Nu-Torque™ yarn of linear density 84.4 tex was produced, its properties were test and compared with conventional ring spinning yarn. In addition, the fabric properties and appearance of denim weaving separately using these two yarns as weft are tested and compared. Hua Tao *et al* (38)

Improvement of Distinguishing Method for Wool Fiber

Improve the bi-class linear discriminatory analysis method base on Fisher criteria. Use improved non-linear method to treat the virtue of the sheep wool and the cashmere. Collect the distinguishing index acquired and make a statistics of discriminatory result. By this the specimen of unknown animal fiber can be distinguished. Shen Jinghu *et al* (40)

Application of Grayscale Morphology in Image Processing of Animal Fibers

The grayscale morphology in image processing technique is applied to animal fiber image. Base on experiments and the reasonable design of the process, it is